Supplementary Information

http://www.rsc.org

Table of Contents

Supplementary Information

1 The Structurally Known Polyaluminum Species and A Classification

The ten finite polyaluminum species shown in the top of Figure S1 fall into two groups: one is characterized by "core-shell" structure derived from the ε-Keggin structure, in which a core of AlO_4 tetrahedron is surrounded by a shell of twelve AlO_6 octahedra linked by vertex- and edge-sharing such as ε-K–Al_{13} (crystallized as $Na[Al_{13}O_4(OH)_{24}(H_2O)_{12}][SO_4]_4\cdot10H_2O$, $Na[Al_{13}O_4(OH)_{24}(H_2O)_{12}]$ $[SeO_4]_4\cdot10H_2O$ and $[Al_{13}O_4(OH)_{25}(H_2O)_{11}][SO_4]_3\cdot16H_2O$ by Johansson et al.),[34-37] S–K–Al_{13} (crystallized as $[Al_{13}O_4(OH)_{25}(H_2O)_{10}(SO_4)][SO_4]_2\cdot5H_2O$ by Sun et al.),[48] a structure similar to the ε-K–Al_{13} but the units are linked by two $(SO_4^{2-})_{0.5}$ with replacement of a H_3O^+ ion, Na–δ-Al_{13} (crystallized as Na–δ-$[Al_{13}O_4(OH)_{24}(H_2O)_{15}][SO_4]_4\cdot16H_2O$ by Rowsell and Nazar),[49] a derivative of ε-K–Al_{13} in which one of the triads (Al_3O_{13}) units which consists of three vertex- and edge-shared AlO_6 octahedra is rotated 60° with respect to the remainder of the ε-K–Al_{13} cluster to form six shared vertexes instead of three edges, and a NaO_6 octahedron caps on the rotated Al_3O_{13} unit, Al_{30} (crystallized as $[Al_{30}O_8(OH)_{56}(H_2O)_{26}][SO_4]_9\cdot xH_2O$ by Rowsell and Nazar, and Allouche et al.),[49, 50] an aggregation of two octahedral AlO_6 monomer capped δ-Al_{13} linked by additional two octahedral AlO_6 monomers via sharing four of its vertexes, in which each monomer capped δ-Al_{13} is formed by capping an AlO_6 octahedral monomer on the rotated triad unit of a δ-Al_{13} by sharing three of its edges, and S–Al_{32} (crystallized as $[Al_{32}O_8(OH)_{60}(H_2O)_{28}(SO_4)_2][SO_4]_7[Cl]_2\cdot30H_2O$ by Sun et al.),[48] a structure similar to that of Al_{30} but the units are linked by two $[Al(OH)_2(H_2O)_3(SO_4)]^-$ groups with replacement of four η^1-H_2O molecules; another is characterized by "plank-suspending" structure in which some AlO_6 octahedra are connected to each other in a vertex- and edge-sharing manner to form a "plank" with some additional AlO_6 octahedral monomers "suspended" on the periphery by vertex-sharing, such as P–Al_{13} (crystallized as $[Al_{13}(OH)_{24}(H_2O)_{24}][Cl]_{15}\cdot13H_2O$ by Seichter et al. and Sun et al., as $[Al_{13}(OH)_{24}(H_2O)_{24}][NO_3]_{15}\cdot9H_2O$ by Gatlin et al. and Wang et al.)[51-54] that has a plank formed by seven AlO_6 octahedra with six additional AlO_6 octahedral monomers suspended on its periphery, Al_8 (crystallized as $[Al_8(OH)_{14}(H_2O)_{18}][SO_4]_5\cdot16H_2O$ by Casey et al.)[55] that has a plank formed by four AlO_6 octahedra with four additional AlO_6 octahedra suspended on it, Al_2 (crystallized as $[Al_2(OH)_2(H_2O)_8][SO_4]_2\cdot2H_2O$ and $[Al_2(OH)_2(H_2O)_8][SeO_4]_2\cdot2H_2O$ by Johansson)[56] which can be regarded as a no suspending case of the "plank-suspending" structure with a plank formed by two AlO_6
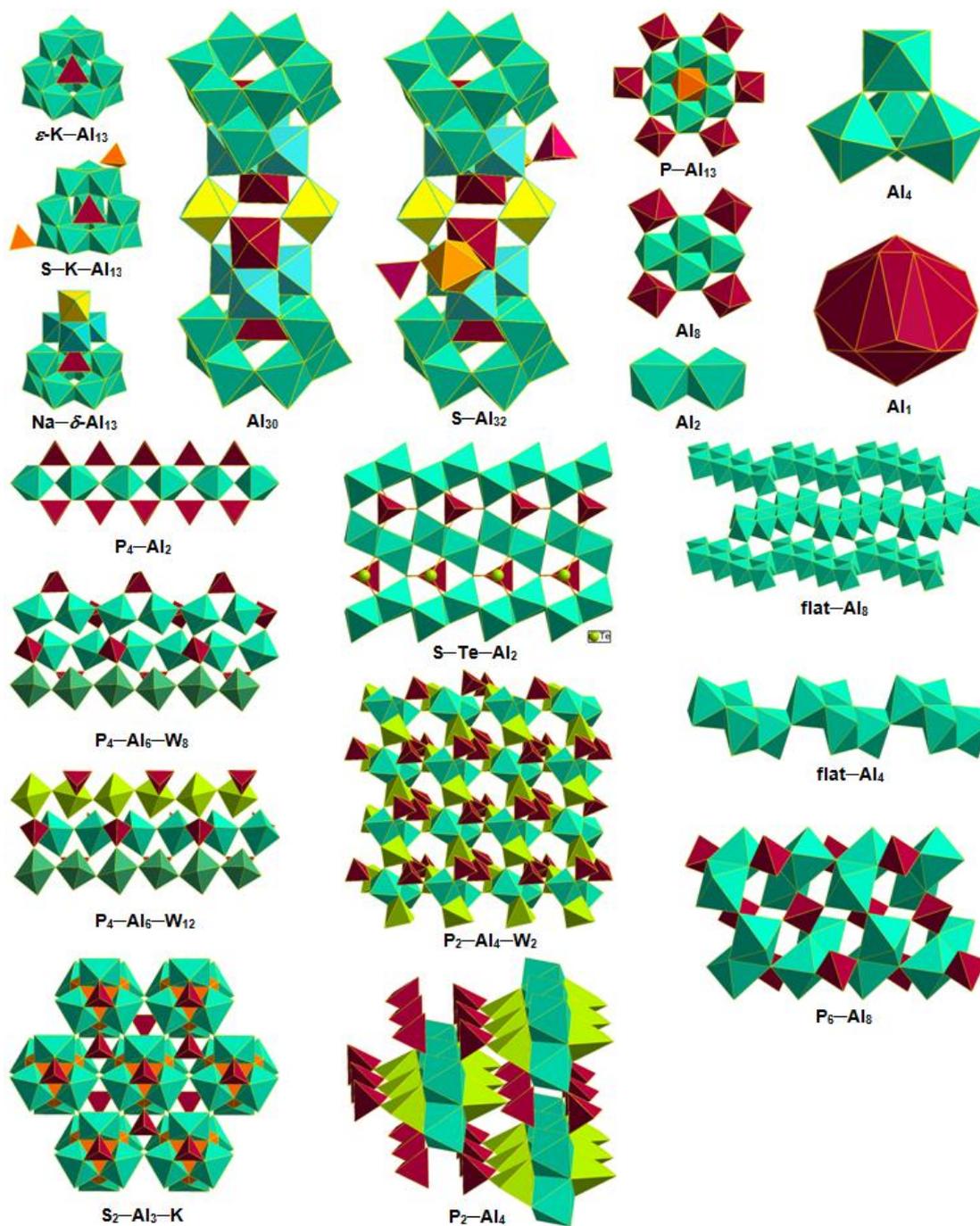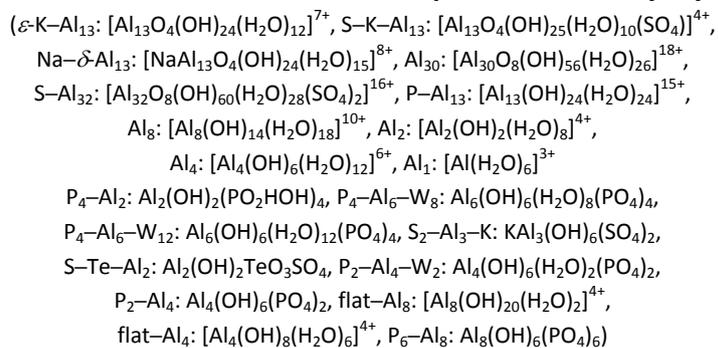
Figure S1. Finite and infinite structures of aluminum species verified by crystal structure analysis

(ε-K–Al$_{13}$: [Al$_{13}$O$_4$(OH)$_{24}$(H$_2$O)$_{12}$]$^{7+}$, S–K–Al$_{13}$: [Al$_{13}$O$_4$(OH)$_{25}$(H$_2$O)$_{10}$(SO$_4$)]$^{4+}$,

Na–δ-Al$_{13}$: [NaAl$_{13}$O$_4$(OH)$_{24}$(H$_2$O)$_{15}$]$^{8+}$, Al$_{30}$: [Al$_{30}$O$_8$(OH)$_{56}$(H$_2$O)$_{26}$]$^{18+}$,

S–Al$_{32}$: [Al$_{32}$O$_8$(OH)$_{60}$(H$_2$O)$_{28}$(SO$_4$)$_2$]$^{16+}$, P–Al$_{13}$: [Al$_{13}$(OH)$_{24}$(H$_2$O)$_{24}$]$^{15+}$,

Al$_8$: [Al$_8$(OH)$_{14}$(H$_2$O)$_{18}$]$^{10+}$, Al$_2$: [Al$_2$(OH)$_2$(H$_2$O)$_8$]$^{4+}$,

Al$_4$: [Al$_4$(OH)$_6$(H$_2$O)$_{12}$]$^{6+}$, Al$_1$: [Al(H$_2$O)$_6$]$^{3+}$

P$_4$–Al$_2$: Al$_2$(OH)$_2$(PO$_2$HOH)$_4$, P$_4$–Al$_6$–W$_8$: Al$_6$(OH)$_6$(H$_2$O)$_8$(PO$_4$)$_4$,

P$_4$–Al$_6$–W$_{12}$: Al$_6$(OH)$_6$(H$_2$O)$_{12}$(PO$_4$)$_4$, S$_2$–Al$_3$–K: KAl$_3$(OH)$_6$(SO$_4$)$_2$,

S–Te–Al$_2$: Al$_2$(OH)$_2$TeO$_3$SO$_4$, P$_2$–Al$_4$–W$_2$: Al$_4$(OH)$_6$(H$_2$O)$_2$(PO$_4$)$_2$,

P$_2$–Al$_4$: Al$_4$(OH)$_6$(PO$_4$)$_2$, flat–Al$_8$: [Al$_8$(OH)$_{20}$(H$_2$O)$_2$]$^{4+}$,

flat–Al$_4$: [Al$_4$(OH)$_8$(H$_2$O)$_6$]$^{4+}$, P$_6$–Al$_8$: Al$_8$(OH)$_6$(PO$_4$)$_6$)

octahedra only, Al_4 & Al_1 (crystallized as $[Al_4(OH)_6(H_2O)_{12}][Al(H_2O)_6]_2Br_{12}$ by Sun *et al.*),[57] the former can be regarded as a no plank case of the "plank-suspending" structure, it is composed of four AlO_6 octahedra that are suspended to each other by sharing three vertexes of each octahedron and form a large regular tetrahedron with ideal T_d symmetry, the central Al^{3+} ion of the latter is coordinated by 6 disordered H_2O molecules, that form a core-shell structure with ideal D_{3d} symmetry and coexist in a 2:1 ratio with the former.

The ten infinite polyaluminum species shown in the bottom of Figure S1 fall into three groups: the first group is characterized by vertex-sharing either between AlO_6 octahedra or between AlO_6 octahedra and counterions (tetrahedral PO_2HOH, PO_4, or SO_4 ligands), such as P_4–Al_2 (crystallized as $Al_2(OH)_2(PO_2HOH)_4·6H_2O$ by Li and Xiang),[58] an one-dimensional infinite chain composed of OH-shared $Al(OH)_2O_4$ octahedra and μ_2-PO_2HOH tetrahedra that locked the intrachain adjacent $Al(OH)_2O_4$ octahedra by O-sharing, P_4–Al_6–W_8 (a natural wavellite mineral crystallized as $Al_6(OH)_6(H_2O)_8(PO_4)_4·2H_2O$ found from USA, its structure was solved by Araki and Zoltai),[59] an incompact three-dimensional infinite structure composed of two types of one-dimensional infinite chains presented in a 1:2 ratio and respectively composed of OH-shared $Al(OH)_2O_2(H_2O)_2$ and $Al(OH)_2O_3(H_2O)$ octahedra, and μ_4-PO_4 tetrahedra that fixed the interspaces between chains by O-sharing, P_4–Al_6–W_{12} (a similar natural wavellite mineral crystallized as $Al_6(OH)_6(H_2O)_{12}(PO_4)_4$ found from China, its structure was solved by Fu),[60] also an incompact three-dimensional infinite structure but composed of three types of one-dimensional infinite chains that are respectively composed of OH-shared $Al(OH)_2O(H_2O)_3$, $Al(OH)_2O_2(H_2O)_2$, and $Al(OH)_2O_3(H_2O)$ octahedra, μ_4-PO_4 and μ_2-PO_4 tetrahedra that fixed the interspaces between chains by O-sharing, S_2–Al_3–K (a natural alunite mineral crystallized as $KAl_3(OH)_6(SO_4)_2$ found from USA and Italy, the structure was respectively solved by Hendricks,[61] Wang et al.,[62] and Menchetti and Sabelli,[63] and a XRD pattern was calculated from Hendricks' parameters by Pabst[64]), a two-dimensional infinite hexameric ring layer composed of OH-shared $Al(OH)_4O_2$ octahedra and O-shared μ_3-SO_4 tetrahedra that coordinate to each Al_3 island formed by three vertex-shared hexameric rings from its two sides, with the K^+ ions locked the interlayer space by forming KO_{12} icosahedra, also, the K^+ position can be replaced by Na^+ or others whole or in part (such as the natroalunite mineral crystallized as $NaAl_3(OH)_6(SO_4)_2$ found from China, the structure was solved from its powder XRD data by Tang et al.;[65] another natroalunite mineral crystallized as $Na_{0.58}K_{0.42}Al_3(OH)_6(SO_4)_2$ found from Japan, the structure was solved by Okada et al.;[66] and the minamiite and ammonioalunite minerals whose structures were solved by Ossaka et al.[67] and

Altaner et al.[68]); the second group is characterized by edge- and vertex-sharing or edge-sharing only, such as S–Te–Al$_2$ (crystallized as Al$_2$(OH)$_2$TeO$_3$SO$_4$ by Johansson and Lindqvist),[69] a two-dimensional infinite sheet formed by splicing one-dimensional infinite zigzag chains together and locked by μ_3-TeO$_3$ pyramids and μ_2-SO$_4$ tetrahedra via O-sharing, while each chain is composed of edge-shared Al$_2$ units that connect together nose to tail by HO–OH edge-sharing, P$_2$–Al$_4$–W$_2$ (a natural senegalite mineral crystallized as Al$_4$(OH)$_6$(H$_2$O)$_2$(PO$_4$)$_2$ found from Senegal, the structure was solved by Keegan et al.),[70] a crisscrossed three-dimensional infinite framework formed from orthogonal one-dimensional infinite chains and μ_4-PO$_4$ tetrahedra that locked the intrachain and interchain spaces by O-sharing, while each chain is composed of (OH)$_2$-edge-shared Al(OH)$_3$O$_2$(OH$_2$) octahedron and Al(OH)$_3$O$_2$ trigonal bipyramid units that link together nose to tail by OH-sharing, P$_2$–Al$_4$ (a natural augelite mineral crystallized as Al$_4$(OH)$_6$(PO$_4$)$_2$ found from USA, the structure was solved by Araki et al.),[71] a three-dimensional infinite framework formed from two-dimensional infinite layers that are composed of Al$_4$ units which are linked together by μ_4-PO$_4$ tetrahedra (three of the four coordinated O atoms are used for each PO$_4^{3-}$ ion) via O-sharing, and the interspaces between layers are also locked by the μ_4-PO$_4$ tetrahedra (the fourth coordinated O atom is used for each PO$_4^{3-}$ ion) via O-sharing, while each Al$_4$ unit are composed of two (OH)$_2$-edge-shared Al(OH)$_4$O$_2$ octahedra and two Al(OH)$_3$O$_2$ trigonal bipyramids connected to its two sides by (OH)$_3$-edges-sharing, also, the P position can be replaced by V (such as the compound crystallized as Al$_4$(OH)$_6$(VO$_4$)$_2$, a similar structure was solved from its powder XRD data by Pecquenard et al.),[72] flat–Al$_8$ (a natural felsobanyaite mineral crystallized as Al$_8$(OH)$_{20}$(H$_2$O)$_2$(SO$_4$)$_2$·6H$_2$O found from Romania, the structure was solved by Farkas and Pertlik),[73] a three-dimensional infinite structure formed by splicing parallel (but with opposite orientation) infinite flat-Al$_8$ chains together by OH-sharing, while each infinite flat-Al$_8$ chain is composed of flat–Al$_8$ units that are linked together nose to tail by edge-sharing, and each flat–Al$_8$ unit are formed by splicing eight AlO$_6$ octahedra into two lines by edge-sharing, in which there is not any SO$_4^{2-}$ ion participating the coordination of the aluminum polycation, and flat–Al$_4$ (a natural aluminite mineral crystallized as Al$_4$(OH)$_8$(H$_2$O)$_6$(SO$_4$)$_2$·8H$_2$O found from Hungary, the structure was solved by Sabelli and Ferroni),[74] in which four AlO$_6$ octahedra are connected each other by edges-sharing forming a flat–Al$_4$ unit, many flat–Al$_4$ units are linked together nose to tail by edge-sharing forming an infinite flat-Al$_4$ chain, again, there is not any SO$_4^{2-}$ ion participating the coordination of the aluminum polycation; the third group is characterized by face- and vertex-sharing, such as P$_6$–Al$_8$ (a natural trolleite mineral crystallized as Al$_8$(OH)$_6$(PO$_4$)$_6$ found from USA, the structure was solved by Moore

and Araki),[75] a very dense three-dimensional infinite structure composed of infinite double-chains that are formed by OH-bridging the Al dimmers that are formed by connecting two AlO_6 octahedra via face-sharing, and μ_4-PO_4 tetrahedra locked the intrachain and interchain spaces by O-sharing.

2 Characterization Results of Other Methods

2.1 XRD Analysis

The XRD patterns of the prepared polyaluminum iodide, bromide and chloride are shown in Figure S2, which were recorded on a Rigaku D/MAX 2500/PC X-ray diffractometer operating at λ=1.54178Å (Cu $K\alpha$), 40kV, 200mA for the former and 300mA for the latter two. The former can not match with any known compound within the latest PDF database and all the diffraction lines can be indexed, indicating that it is a new phase with high purity, its formula $Al(OH)_2I\cdot2H_2O$ was measured by chemical analysis (see next section). The latter two can well match with the reported XRD lines (blue) of $Al(OH)_2Br\cdot2H_2O$ on PDF27-005 and $Al(OH)_2Cl\cdot2H_2O$ on PDF27-012, respectively, not only for their peak positions but also for their relative intensities, indicating that the purity of so prepared product $Al(OH)_2Br\cdot2H_2O$ and $Al(OH)_2Cl\cdot2H_2O$ are also high. Several unidentified weak peaks on higher 2ϑ region in Fig. S2 B and C are included in our indexing results, so they are not impurity peaks.
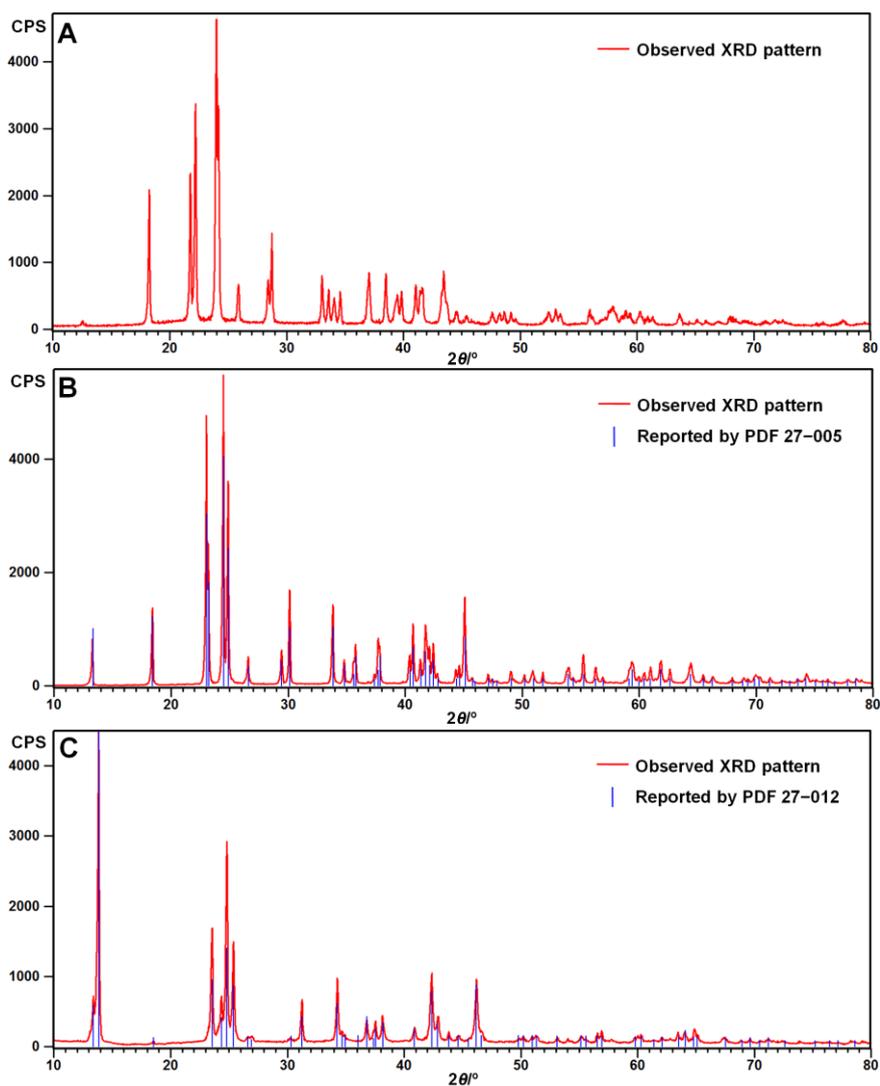
Figure S2. The XRD patterns of the prepared polyaluminum iodide (A), bromide (B) and chloride (C)

2.2 Chemical Analysis

The prepared polyaluminum iodide is watersoluble, so the dry sample was dissolved in deionized water directly and was depolymerized by adding concentrated HNO_3 and boiling for 1 minute. The prepared polyaluminum bromide is waterinsoluble, the dry sample was dissolved in a NaOH solution (5mol/L) and kept boiling for 5 minutes, then the strongly alkaline solution was cooled down to room temperature and was adjusted to be highly acidic by adding a HNO_3 solution (1:1 volume ratio) to depolymerize the polyaluminum compound. The amount of Al^{3+} ion was measured by the EDTA inverse titration method, I^- anion was measured by the oxidimetry, Br^- anion was measured by Fajans method, OH^- anion was calculated from the electric neutrality principle, and H_2O was calculated by

the weight subtraction method. The yield was calculated through dividing the obtained product weight by the expected product weight according to the reaction equation. The analysis results are listed in Table S1.

Table S1. The chemical analysis results of the prepared polyaluminum compounds

sample	polyaluminum iodide				polyaluminum bromide			
component	Al^{3+}	I^-	OH^-	H_2O	Al^{3+}	Br^-	OH^-	H_2O
calculated content*/%	12.05	56.67	15.19	16.09	15.25	45.16	19.22	20.36
measured content/%	12.08	56.64	15.25	16.03	15.24	45.25	19.19	20.32
content/mmol g^{-1})	4.477	4.463	8.967	8.896	5.648	5.663	11.28	11.28
mole ratio	1.000	0.997	2.003	1.987	1.000	1.003	1.997	1.997
whole number ratio	1	1	2	2	1	1	2	2
formula	$Al(OH)_2I\cdot2H_2O$				$Al(OH)_2Br\cdot2H_2O$			
yield/%	76.3				71.9			

*It means that the percentage compositions are calculated from the formulas $Al(OH)_2I\cdot2H_2O$ and $Al(OH)_2Br\cdot2H_2O$, respectively.

From Table S1 it is obvious that the measured percentage compositions are very close to those calculated from their formulas and the mole ratios are very close to whole numbers, indicating that the formulas determined by chemical analysis are correct (the formula of the polyaluminum bromide is in accordance with that reported by PDF27-005) and the purities of so prepared compounds are high. These results are in good agreement with the results of XRD analysis.

2.3 Thermal Analysis

The TG curves of the prepared $Al(OH)_2I\cdot2H_2O$ and $Al(OH)_2Br\cdot2H_2O$ were recorded on a Netzsch STA 409PC thermal analyzer. The temperature was risen at a speed of 2.5℃/min in the range of room temperature to 1200℃ with a N_2 velocity of flow of 20mL/min. The results are shown in Figure S3. There are two mass loss steps on each TG curve, the total mass loss are 77.50% and 71.62% for the iodide and bromide, respectively, which are in good conformity with the calculated values of 77.23% and 71.19% from their formula, indicating that the purities of the prepared compounds are well and the formula measured by chemical analyses are correct. It is difficult to match each mass loss step

with an exact thermolysis reaction, because the final decomposition products are Al_2O_3 for these two compounds and the escapes of HI, HBr, and H_2O gases are always accompanied in the whole thermolysis process. The overall thermolysis equation is: $2Al(OH)_2X \cdot 2H_2O \rightarrow Al_2O_3 + 2HX\uparrow + 3H_2O\uparrow$ (X = I, Br).
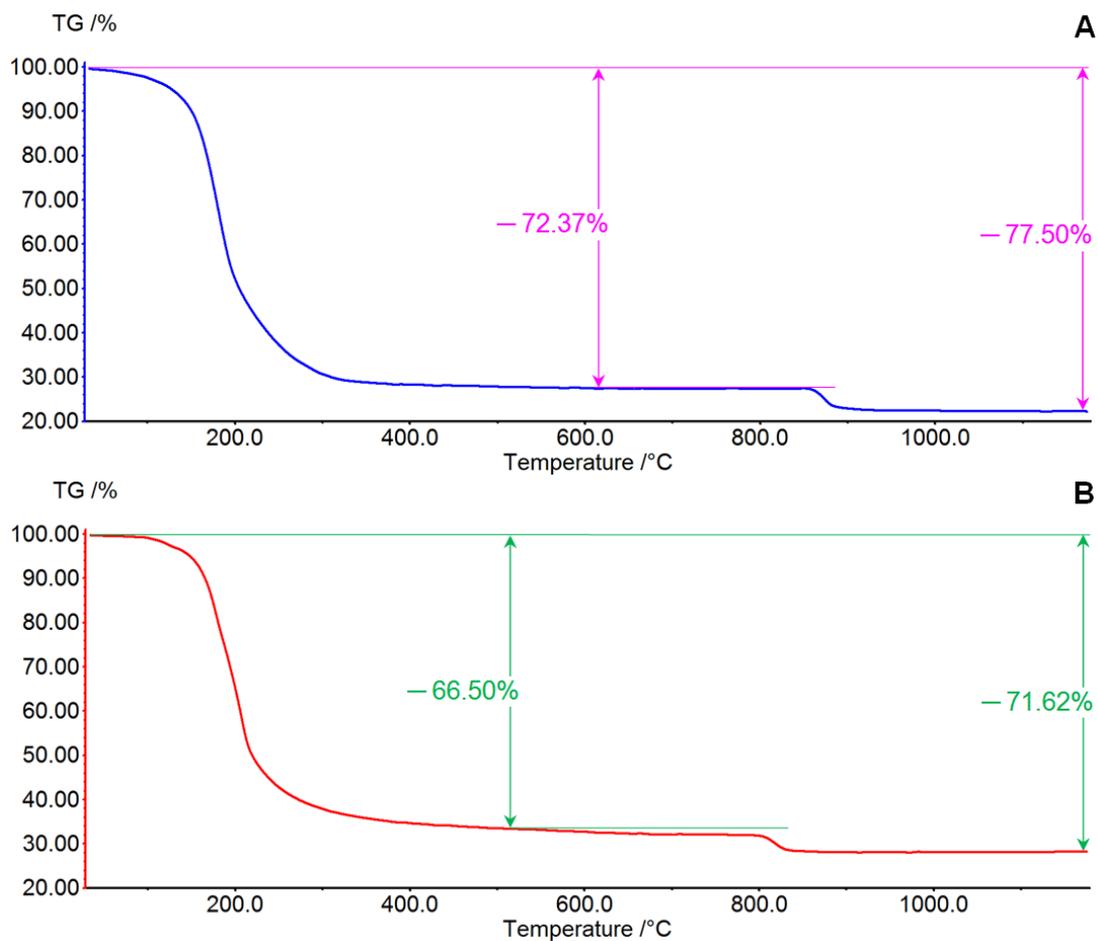
Figure S3. The TG curves of the prepared $Al(OH)_2I \cdot 2H_2O$ (A) and $Al(OH)_2Br \cdot 2H_2O$ (B)

3 Rietveld Full-profile Fitting Results Based on Le Bail Fit

It is obvious that the *R* indexes are low and the GOF values are very close to 1, indicating that the indexing results for these three compounds are reliable, and the *HKL* files generated by the program can be used for structure solving.
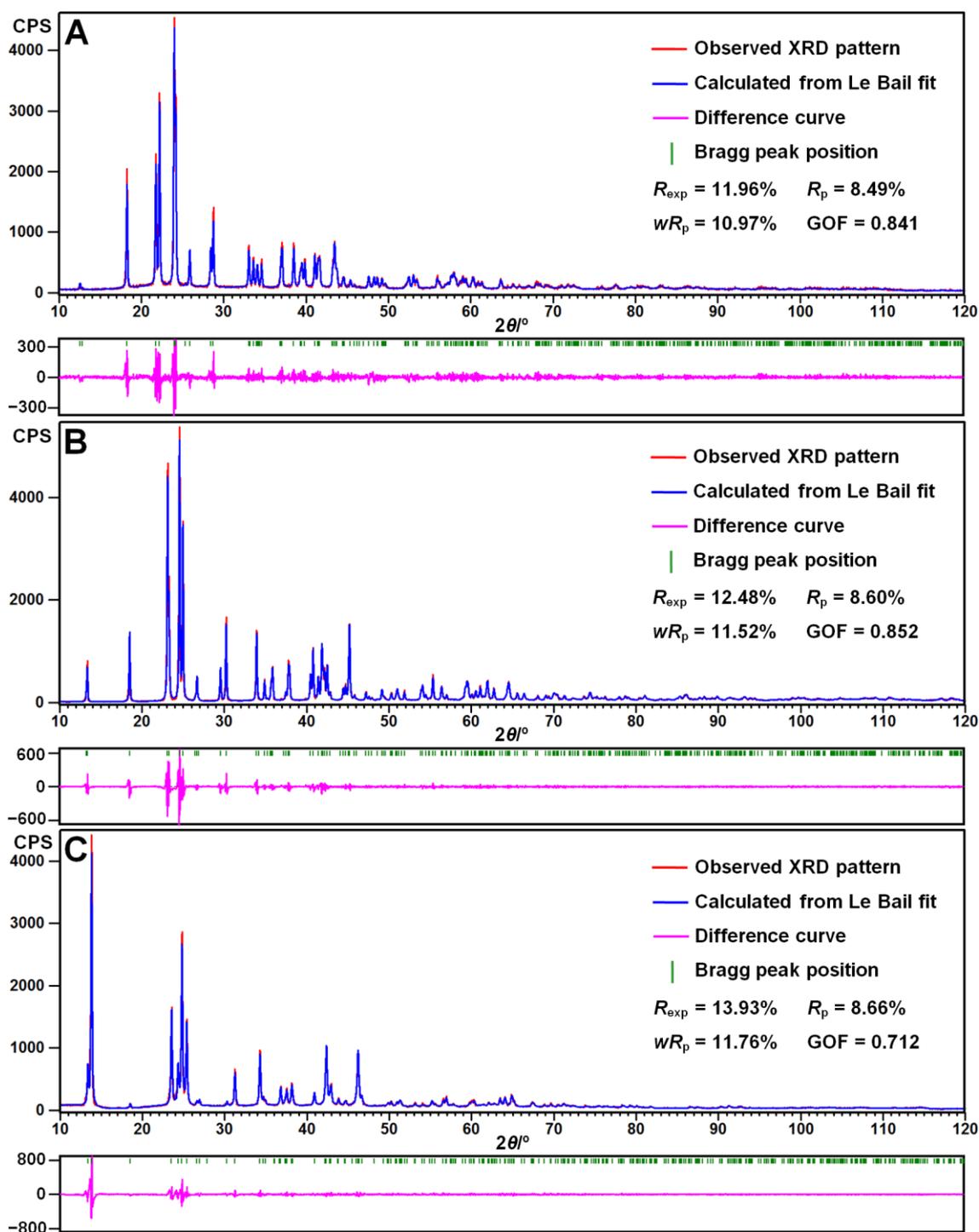
Figure S4. Rietveld full-profile fitting results based on Le Bail fit for the prepared $Al(OH)_2I \cdot 2H_2O$ (A), $Al(OH)_2Br \cdot 2H_2O$ (B), and $Al(OH)_2Cl \cdot 2H_2O$ (C)
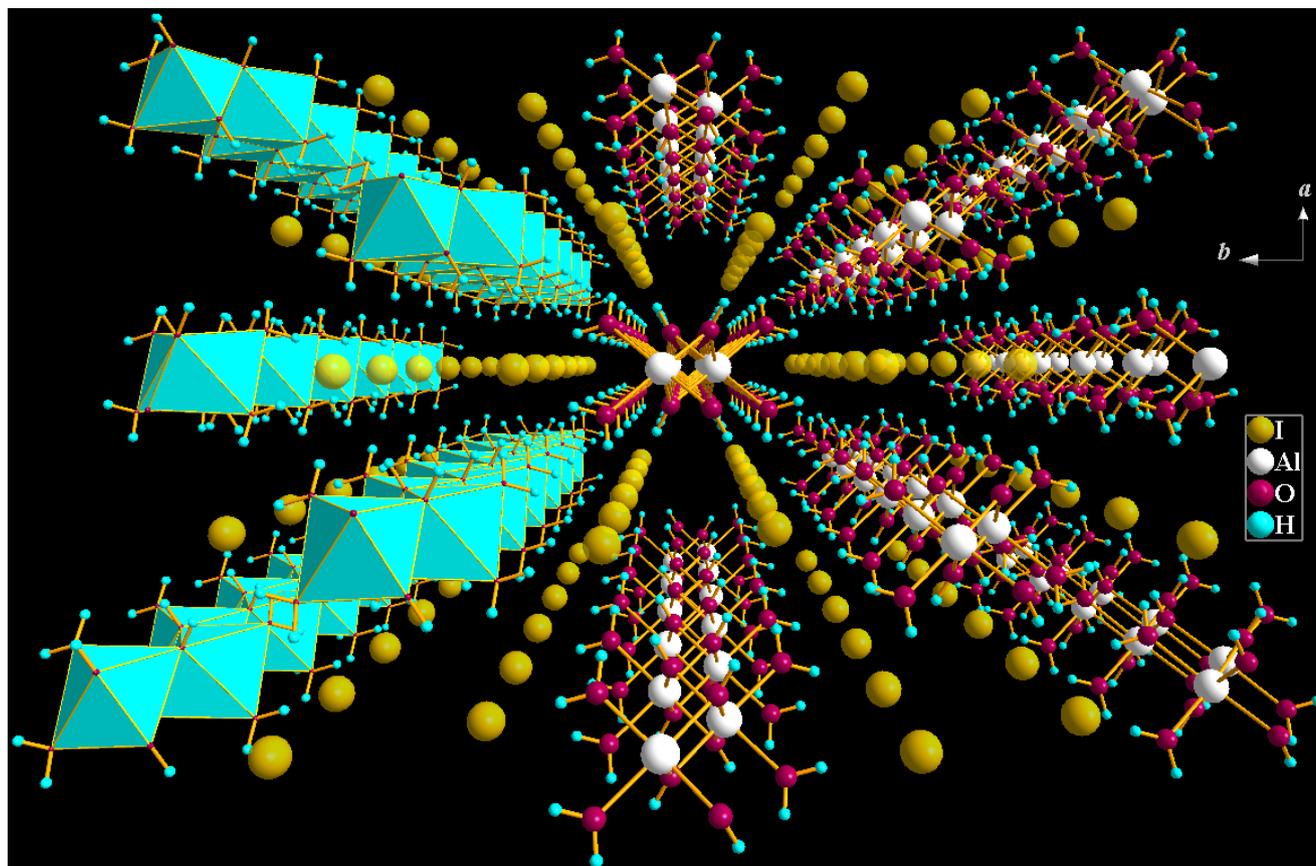
4 Three-dimensional View of The Crystal Structure of $Al_2(OH)_4(H_2O)_4I_2$

Figure S5. A three-dimensional view of the crystal structure of $[Al_2(OH)_4(H_2O)_4]I_2$ along the c direction

(Left: polyhedral representation; Right: ball and stick representation)

5 Infinite Chain Structures of the Polycation $[Al_2(OH)_4(H_2O)_4]^{2+}$ in $[Al_2(OH)_4(H_2O)_4]X_2$
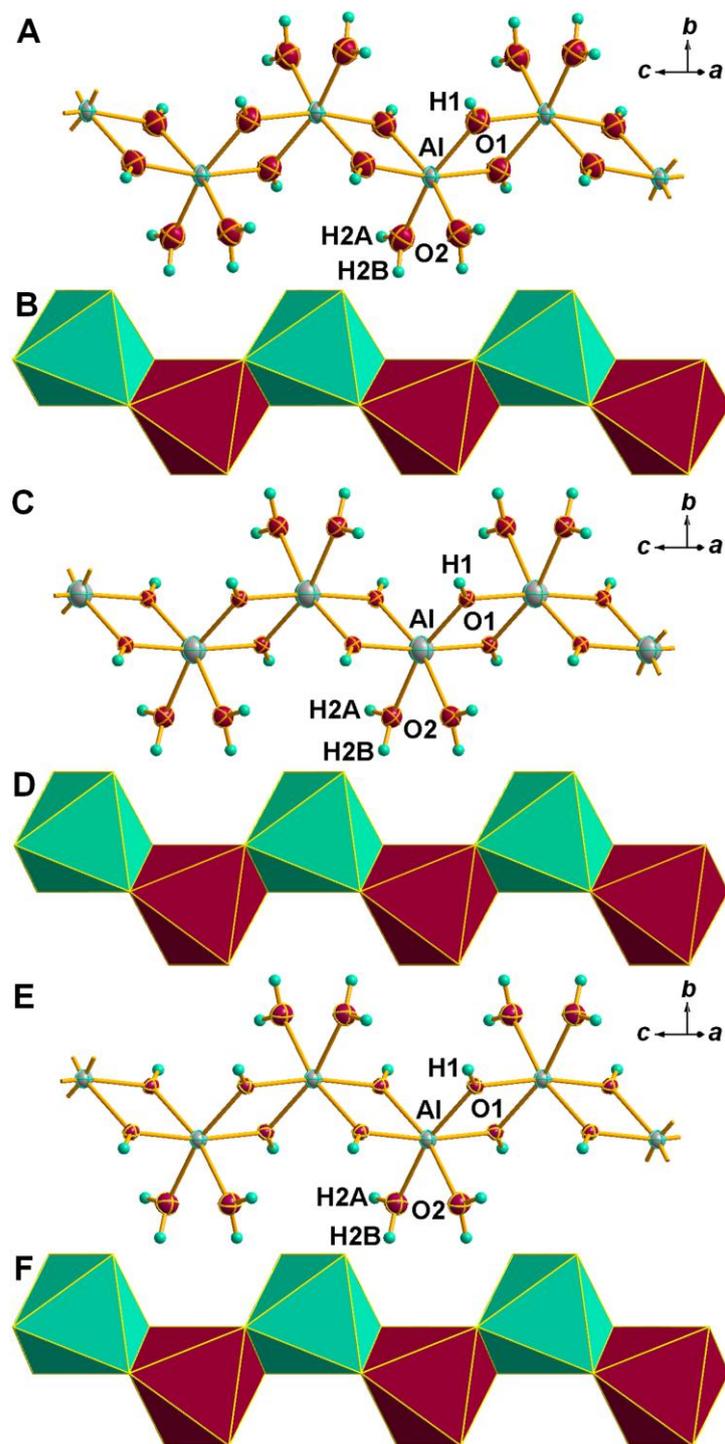
Figure S6. Infinite chain structures of the polycation $[Al_2(OH)_4(H_2O)_4]^{2+}$ in $[Al_2(OH)_4(H_2O)_4]X_2$ [X = I (A-B), Br (C-D), and Cl (E-F)]: (A), (C) and (E) ellipsoid-stick representations with a probability of 80%, (B), (D) and (F) polyhedral representations viewed along the (101) direction. The cyan and magenta octahedra represent two types of AlO_6 octahedra with inverse orientations.

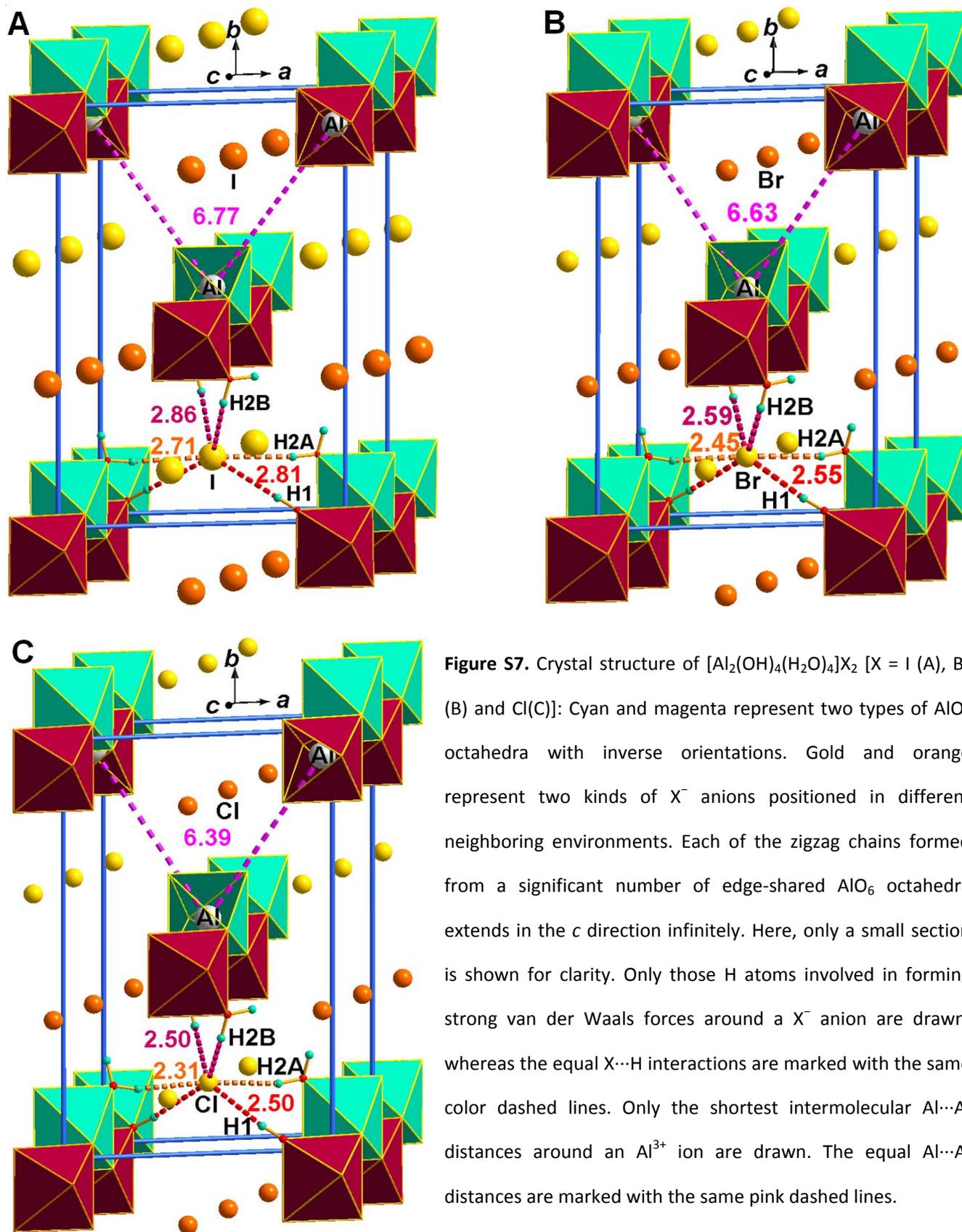## 6 The Crystal Structures and Intermolecular Interactions of $[Al_2(OH)_4(H_2O)_4]X_2$

Figure S7. Crystal structure of $[Al_2(OH)_4(H_2O)_4]X_2$ [X = I (A), Br (B) and Cl(C)]: Cyan and magenta represent two types of AlO_6 octahedra with inverse orientations. Gold and orange represent two kinds of X^- anions positioned in different neighboring environments. Each of the zigzag chains formed from a significant number of edge-shared AlO_6 octahedra extends in the *c* direction infinitely. Here, only a small section is shown for clarity. Only those H atoms involved in forming strong van der Waals forces around a X^- anion are drawn, whereas the equal X⋯H interactions are marked with the same color dashed lines. Only the shortest intermolecular Al⋯Al distances around an Al^{3+} ion are drawn. The equal Al⋯Al distances are marked with the same pink dashed lines.

7 XRD Pattern of The Product Precipitated from Treated Solution of Al$_2$(OH)$_4$(H$_2$O)$_4$I$_2$ at 75℃

The XRD pattern of the product precipitated from the treated solution of Al$_2$(OH)$_4$(H$_2$O)$_4$I$_2$ at 75℃ in a steel reactor with a Teflon inner container for two weeks is shown in Figure S8, which was recorded on a PANalytical Empyrean X-ray diffractometer operating at λ=1.54178Å (Cu-Kα), 40kV, and 40mA. From Figure S8 it is clear that the observed pattern can well match with the reported XRD lines of gibbsite (lime) on PDF74-1775 and nordstrandite (fuchsia) on PDF72-623,[116, 117] not only for their peak positions but also for their relative intensities, and no any residue line left, indicating that the product is a mixture of two types of Al(OH)$_3$. After a Rietveld full-profile fitting based on their structures, a composition of 59% nordstrandite and 41% gibbsite is obtained with quite good R indexes and GOF value, implying that the phases quantitative analysis result is believable.
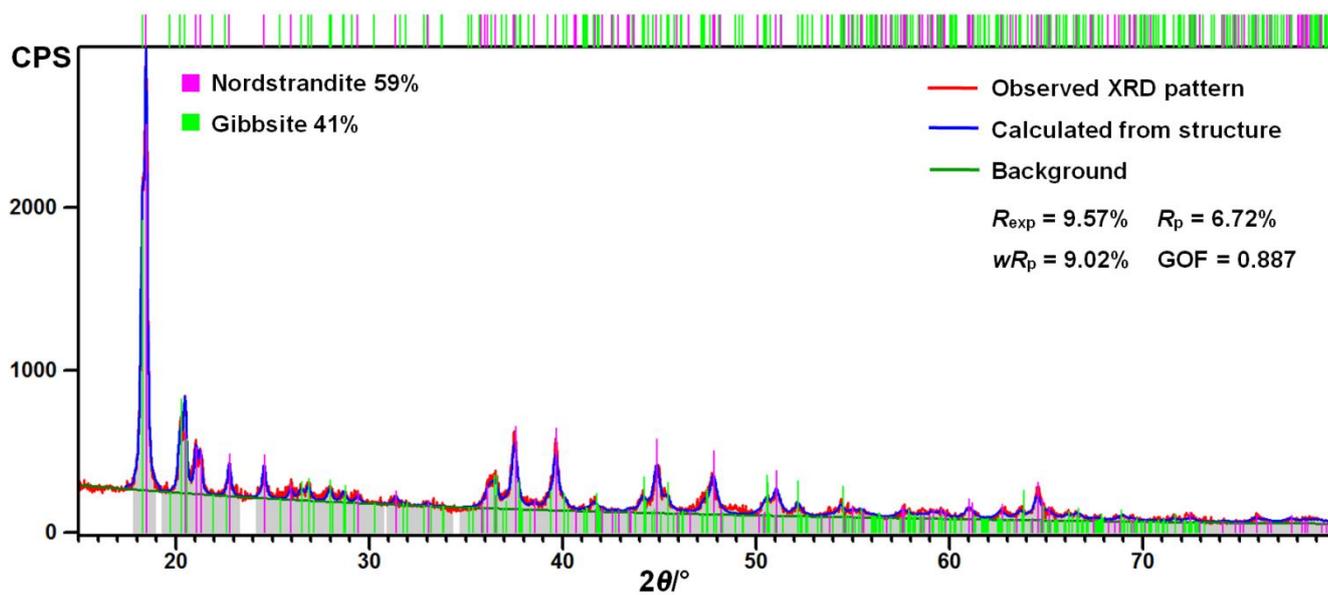

Figure S8. XRD pattern of the mixture precipitated from treated solution of Al$_2$(OH)$_4$(H$_2$O)$_4$I$_2$ at 75℃